Applied Physics Letters

Pure spin current phenomena

Cite as: Appl. Phys. Lett. **117**, 190501 (2020); https://doi.org/10.1063/5.0032368
Submitted: 07 October 2020 . Accepted: 28 October 2020 . Published Online: 09 November 2020

S. Y. Huang, D. Qu, T. C. Chuang, C. C. Chiang, W. Lin, and C. L. Chien

Applied Physics Letters PERSPECTIVE scitation.org/journal/apl

Pure spin current phenomena

Cite as: Appl. Phys. Lett. **117**, 190501 (2020); doi: 10.1063/5.0032368
Submitted: 7 October 2020 · Accepted: 28 October 2020 ·
Published Online: 9 November 2020

View Online Export Citation CrossMark

S. Y. Huang,[1] D. Qu,[2] T. C. Chuang,[1] C. C. Chiang,[1] W. Lin,[3] and C. L. Chien[1,3,a)]

AFFILIATIONS

[1]Department of Physics, National Taiwan University, Taipei 10617, Taiwan
[2]Institute of Physics, Academia Sinica, Taipei 11529, Taiwan
[3]Department of Physics and Astronomy, Johns Hopkins University, Baltimore, Maryland 21218, USA

[a)]Author to whom correspondence should be addressed: clchien@jhu.edu

ABSTRACT

Spintronic phenomena and devices have evolved from exploiting spin-polarized current to pure spin current. A pure spin current can more efficiently deliver spin angular momentum with fewer or no charge carriers, enabling spin–orbit torque switching in ferromagnets. The prospects of antiferromagnetic spintronics, especially electrical switching, remain perplexing and controversial. We describe some recent advances, outstanding issues, challenges, and prospects of pure spin current.

INTRODUCTION

Spintronic phenomena and devices have evolved from exploiting spin-polarized current to pure spin current. A pure spin current has the unique attribute of delivering spin angular momentum efficiently with a minimal of charge carriers in metals and no charge carriers at all in insulators. The spin Hall effect (SHE),[1–3] spin pumping (SP),[4] and longitudinal spin Seebeck effect (LSSE)[5] in conjunction with heavy metals (HMs), ferromagnetic (FM) and antiferromagnetic (AF) metals, and insulators can generate pure spin currents. Importantly, pure spin current enables spin–orbit torque (SOT),[6–8] a mechanism different from spin transfer torque (STT),[9,10] to switch FM entities, essential for high-density memory devices, such as magnetic random-access memory (MRAM). However, there are also perplexing aspects in pure spin current phenomena in FMs and especially in AF entities. In this Perspective, we mention some recent advances, outstanding issues, challenges, and prospects of pure spin current.

GENERATION OF PURE SPIN CURRENT

A charge current $\boldsymbol{j}_C$ in a HM can generate a pure spin current of[1–3]

$$\boldsymbol{j}_S = (\hbar/2e)\theta_{SH}\,\boldsymbol{j}_C \times \boldsymbol{\sigma} \quad (1)$$

in the lateral direction with the spin index $\boldsymbol{\sigma}$ in the third direction, known as the SHE. The spin Hall angle θ_{SH}, which specifies the charge-to-spin conversion efficiency, may be positive (e.g., Pt and Au) or negative (e.g., W and Ta) with $|\theta_{SH}| \leq 1$.[11,12] Since spin–orbit coupling (SOC) increases with the atomic number, many 4*d* and 5*d* HMs have large θ_{SH}. While some 3*d* metals have negligibly small (e.g., Cu), others (e.g., Cr and Ni) have substantial θ_{SH}.[13–15]

In the LSSE in HMs/FMs, one uses a temperature gradient, whereas in SP, one uses ferromagnetic resonance (FMR), to inject a pure spin current into a HM with $\boldsymbol{\sigma}$ set by the magnetization direction of the FM, as shown in Fig. 1. The resultant pure spin current in the HM can be indirectly detected after conversion through the inverse spin Hall effect (ISHE) to a charge current, often detected as a DC voltage. As such, the electrical measurements for spin-to-charge conversion may include unintended charge current effects. The identification and elimination of the accompanying charge current effects are key challenges in pure spin current phenomena.

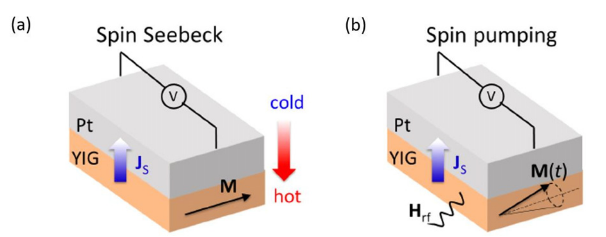

FIG. 1. Schematics of (a) the longitudinal spin Seebeck effect and (b) spin pumping in Pt/YIG, where the direction of the pure spin current $\boldsymbol{j}_S$, the spin index $\boldsymbol{\sigma}$ set by the YIG magnetization, and the inverse spin Hall effect voltage are mutually perpendicular.

LONGITUDINAL SPIN SEEBECK EFFECT

Consider the well-known HM/Py bilayers in the context of the LSSE, where Py = Permalloy = $Ni_{80}Fe_{20}$ is a common FM metal. Under an out-of-plane temperature gradient ($\nabla_z T$) in HM/Py administered by a temperature difference of about 10 K, the LSSE may inject $\boldsymbol{j}_S \,||\, \nabla_z T$ from Py into the HM and be detected by the ISHE $\boldsymbol{E}_{ISHE} \propto \boldsymbol{j}_S \times \boldsymbol{\sigma}$, with $\boldsymbol{\sigma} \,||\, \boldsymbol{M}$ of Py. Even though the measured voltage in the LSSE in Pt/Py and W/Py has the expected field dependence, as shown in Fig. 2(a), it is not the ISHE, because the voltages reveal the same sign for Pt and W, which have θ_{SH} of opposite sign. In fact, neither result comes mainly from spin-to-charge conversion; instead, it is due to the anomalous Nernst effect (ANE), a well-known charge current effect in the Py metal that generates $\boldsymbol{E}_{ANE} \propto \boldsymbol{j}_C \times \boldsymbol{\sigma}$, with $\boldsymbol{j}_C \,||\, \nabla_z T$.[16,17] In the results in Fig. 2(a), there is negligible spin-to-charge conversion in HM/Py, where the ANE in Py overwhelms. The removal of the large ANE contribution in the FM metal is non-trivial.[16–22]

In contrast, the LSSE can be realized in HM/yttrium iron garnet (YIG) with a ferrimagnetic insulator (FMI) yttrium iron garnet (YIG = $Y_3Fe_5O_{12}$) with no charge carriers.[5] The ISHE voltages, as shown in Fig. 2(b), show opposite signs in Pt and W and, furthermore, vanish when a 2-nm-thick MgO layer blocks the spin current injection. Most explorations of pure current effects using the LSSE have employed the FMI, such as YIG, yielding positive θ_{SH} (Pt, Au, etc.) and negative θ_{SH} (Ta, W, etc.) all with $|\theta_{SH}| < 1$,[12] but not FM metals, such as Py.

SPIN PUMPING

In contrast, most SP experiments employ FM metals as in HM/Py, where one uses FMR to inject $\boldsymbol{j}_S$ into the HM and detected via the ISHE.[23] However, there are other complications, including rectification due to the anomalous Hall effect (AHE) and anisotropic magnetoresistance (AMR), the ANE due to FMR heating induced thermal gradients, and other parasitic effects, which have been well documented, but often not taken into account.[24–26] The measured voltage attributed to spin-to-charge conversion lead a wide range of θ_{SH} values spanning as much as two orders of magnitude, some of opposite signs of the same HM.[27–30] SP in NiFe/Ag/Bi shows that Bi/Ag has larger spin-to-charge conversion efficiency than Pt.[31] In contrast, the LSSE in Bi/Ag/YIG shows negligible spin-to-charge conversion in Ag/Bi.[32] The use of the FM metal in SP experiments greatly complicates the spin-to-charge extraction because of the various charge effects.

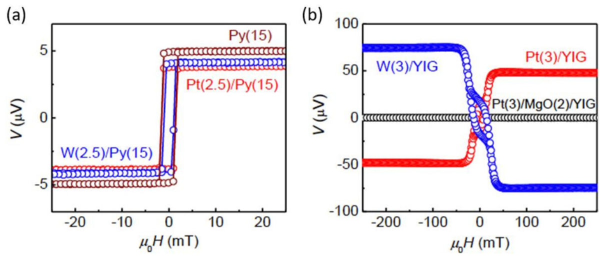

FIG. 2. (a) Magnetic field dependence of voltages in Py(15), Pt(2.5)/Py(15), and W(2.5)/Py(15) films at room temperature under a vertical temperature difference of $\Delta T = 10$ K applied between the film surface and the bottom of the 0.5 mm thick SiOx/Si substrate. (b) Magnetic field dependence of voltage in the Pt(3)/YIG, W(3)/YIG, and Pt(3)/MgO(2)/YIG samples at room temperature under $\Delta T = 10$ K applied between the film surface and the bottom of the 0.5 mm thick polycrystalline YIG slab. The numbers in parentheses are thicknesses in nm.

The SP experiments in HM/YIG, although free of the charge effects such as the ANE, pose other complications. The FMR microwaves, which enable SP, also excite various spin-wave resonance (SWR) modes that can also inject pure spin currents and give rise to ISHE voltages.[33] The signals from these SWR modes may be separated and extracted in thick (>50 μm) YIG crystals, but not in thin YIG layers (< a few μm), where the SP and SWR signals are unresolved.[34] Attributing the signals entirely to that of spin-to-charge, as is often done, could greatly exaggerate the SP contribution. It has been found that SWR modes in YIG are more efficient for spin current generation than that of FMR.[33,34]

Furthermore, the magnitude of spin current generated by SP depends strongly on the quality of the spin injector (e.g., YIG). The SP-induced spin current from polycrystalline YIG films is two-orders-of-magnitude smaller than that from epitaxial YIG films. In contrast, the LSSE excited spin current is surprisingly insensitive to YIG films, epitaxial or polycrystalline.[35] This is because SP relies on collective motions of many magnetic moments driven by FMR, whereas the LSSE is due to incoherent thermally injected magnons with a long magnon diffusion length. In this respect, the robust spin current generated by the LSSE provides superior advantages to exploring spin Hall materials, not only in heavy 5*d* metals of Pt, Ta, W, and Au[12,36] but also in 3*d* metals of Py,[13] Co,[37] and Cr.[15] Furthermore, one can tune θ_{SH} in alloy systems and realize enhancement of spin current through spin fluctuation in AF insulators[38] and spin glass.[39] The discovery by the LSSE of the large ISHE in 3*d* magnets, ferromagnets and antiferromagnets, opens avenues for spin current explorations, including SOT switching.

PROSPECT OF COHERENT SPIN INJECTION

Spin injection in the LSSE is due to thermal magnons, which are inherently incoherent, and as such, the resultant ISHE decreases sharply with the decreasing number of magnons at low temperatures and vanishes at $T \approx 0$ K. On the other hand, SP may be the only scheme that could potentially administer coherent spin injection as first suggested by theory.[4] The prospect of coherent SP has been described in a $T = 0$ K theoretical model, which has been used in analyzing many of the SP experiments at room temperature. A telltale sign of coherent spin current can be unequivocally established by SP experiment at low temperatures. There have been several SP experiments at low temperatures in HM/YIG using thin YIG films or bulk YIG crystals.[34,40] These SP results show vanishingly small ISHE voltages as T approaches 0 K, similar to those in the LSSE. The realization of coherent SP at low temperature remains an experimental challenge.

SPIN–ORBIT TORQUE SWITCHING OF FERROMAGNETIC ENTITIES

The transport of spin angular momentum of electrons can be exploited to switch magnetic entities. The discovery of STT earlier allows current switching of two-terminal giant magnetoresistance (GMR) and magnetic tunnel junction (MTJ) devices.[41] When current density exceeds the switching threshold, the polarity of the current through the device sets the final low (the parallel state) or high (the antiparallel) resistant states. However, the high switching current densities through the device may threaten its integrity due to electromigration and other irreversible changes.

The advent of pure spin current enables SOT provide another switching mechanism in three-terminal FM/HM devices, where the switching current passes through the HM layer, peripheral to the vulnerable multilayer stack, thus mitigating the potential damage to the device. The Landau–Lifshitz–Gilbert (LLG) equation including the SOT is[8,42]

$$\frac{\partial \boldsymbol{M}}{\partial t} = -\gamma \boldsymbol{M} \times H + \frac{\alpha}{M}\boldsymbol{M} \times \frac{\partial \boldsymbol{M}}{\partial t} + a\boldsymbol{M} \times \boldsymbol{\sigma} + b\boldsymbol{M} \times (\boldsymbol{\sigma} \times \boldsymbol{M}), \quad (2)$$

where the first two terms are the precession term and the damping term. The SOT has two terms, the field-like torque $\boldsymbol{\tau_{FL}} = a\boldsymbol{M} \times \boldsymbol{\sigma}$ and the damping-like torque $\boldsymbol{\tau_{DL}} = b\boldsymbol{M} \times (\boldsymbol{\sigma} \times \boldsymbol{M})$, with effective fields, $\boldsymbol{H_{FL}} \sim \boldsymbol{\sigma}$ and $\boldsymbol{H_{DL}} \sim \boldsymbol{\sigma} \times \boldsymbol{M}$, respectively. As described by the LLG equation and demonstrated in several experiments, SOT can readily switch a FM layer with in-plane magnetic anisotropy (IMA),[7,43] but not the FM with perpendicular magnetic anisotropy (PMA).[44,45] This is because the spin current generated by the SHE has its spin index $\boldsymbol{\sigma}$ parallel to the interface and perpendicular to the magnetization, thus incapable of switching a PMA layer. An additional magnetic field along $\boldsymbol{j_C}$ can break the up/down symmetry and readily enable SOT switching of the PMA layer but unsuitable for viable devices.

To achieve field-free switching of the PMA layer, one may employ various schemes to break the symmetry, including altering the physical shape of the FM layer,[46,47] incorporating additional magnetic field from exchange bias or another FM layer.[48–50] One novel scheme is to alter the microstructure of the layer as accomplished in the deterministic field-free switching in Cr/CoFeB/MgO heterostructures with PMA.[51] As a result of the off-axis sputtering, a slanted columnar microstructure is created due to the oblique angle deposition and the shadowing effect as shown in Fig. 3(a). The direction of the tilt angle in the columnar microstructure dictates the polarity of the field-free SOT switching, as shown in Fig. 3(b). One notes that the Cr layer delivers a comparable switching efficiency as that of the 5*d* Ta-based heterostructure, illustrating that 3*d* materials can exhibit large θ_{SH}.

SOT switching can also estimate θ_{SH} assuming switching is due entirely to pure spin current $\boldsymbol{j_S}$. Notably, very large θ_{SH} values have been reported from SOT using topological insulators, such as $(Bi_{0.5}Sb_{0.5})_2Te_3$ (>140),[52] $Bi_{0.9}Sb_{0.1}$ (~52),[53] Bi_xSe_{1-x} (~18),[54] which are also some of the best thermoelectric materials with pronounced thermal responses.

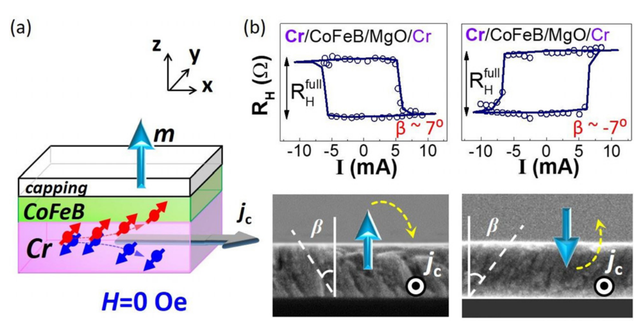

FIG. 3. (a) Schematics of field-free spin–orbit torque (SOT) magnetization switching by applying charge current ($\boldsymbol{j_C}$) in a heterostructure with perpendicular magnetization ($\boldsymbol{m}$). (b) Polarity-controlled field-free SOT switching in Cr/CoFeB/MgO/Cr heterostructures with the opposite tilt angle (β) of oblique columnar structures. Reproduced with permission from Chuang *et al.*, Phys. Rev. Appl. **11**, 061005 (2019). Copyright 2019 American Physical Society.

To date, only FM materials have been exploited for application in field sensing, memory, and other applications. The magnetization of the FM entities that stores the information can be decisively manipulated by a magnetic field, STT, and SOT and unequivocally detected by various techniques from magneto-transport to magnetometry. The two memory (magnetic) states are switched (or written) at high current, but sensed (or read) at low current, which are the prerequisites for electrically controlled spintronic devices. By the same token, devices based on FM entities are also vulnerable to the external magnetic field and stray field interference, especially in high-density memories, such as MRAM.

PROSPECT OF ELECTRICAL SWITCHING OF ANTIFERROMAGNETS

Antiferromagnetic (AF) materials with no net magnetization would be immune to field interference, but the manipulation AF and the detection of the AF ordering are major challenges. In the last few years, there were theoretical suggestions and experimental claims of electrical switching of AF Néel vector. Recent experiments have seriously questioned its validity.

The novel proposal of electrical switching of the AF Néel vector is based on SOT switching, with detection via anisotropic magnetoresistance (AMR) and planar Hall effect (PHE) in conductors or spin Hall magnetoresistance (SMR) in HM-capped insulators. First of all, one cannot easily verify the existence or absence of the Néel vector in any AF materials, especially in thin films. Furthermore, the AMR, PHE, and SMR detection have been established only in detecting FM entities. Most AF switching studies have employed multi- (four or eight) terminal patterned structures, intended to detect the switching of the AF Néel vector with 90° reorientations. AF switching was first reported in metallic epitaxial thin films of CuMnAs[55] and later Mn_2Au,[56] both of which lack inversion symmetry, due to the proposed mechanism of Néel SOT without a HM layer. Later reports claim AF switching in HM/AF bilayers, such as Pt/NiO,[57] Pt/CoO,[58] and Pt/Fe_2O_3,[59,60] where the HM supplies the spin current for the SOT exerted on the adjacent insulating AF oxide layer.

However, the AF switching behavior is entirely different from the known SOT and STT switching in FMs. As shown in Figs. 4(c) and 4(e), each current pulse from both orthogonal pairs of leads for the heterostructure of Pt/NiO creates the same and reversed incremental resistance change (including the incremental changes of Hall resistance ΔR_{XY} and longitudinal resistance ΔR_{XX}).[61] In sharp contrast, there is no change in either STT or SOT switching in FM entities after the current density has exceeded the critical value, regardless of the duration of the current or the number of current pulses.

The cumulative resistance changes have been attributed to multidomain switching, resulting in incremental resistance increases with a series of current pules. However, the observation of the same recurring patterns in the resistance change in the patterned metallic Pt layer, without the AF NiO layer as shown in Figs. 4(d) and 4(f), is astonishing and illuminating.[61] The recurring resistance change could not have been the conclusive evidence of SOT switching of AF. This nonmagnetic resistance change comes from anisotropic thermal gradients [Figs. 4(a) and 4(b)], non-uniform Joule heating,[61] and magnetoelastic stresses,[59] the unintended consequences of the multi-terminal patterned structure.[62,63] One notes that the AF switching events were under enormous current densities (~5 × 10^7 A/cm^2), near the

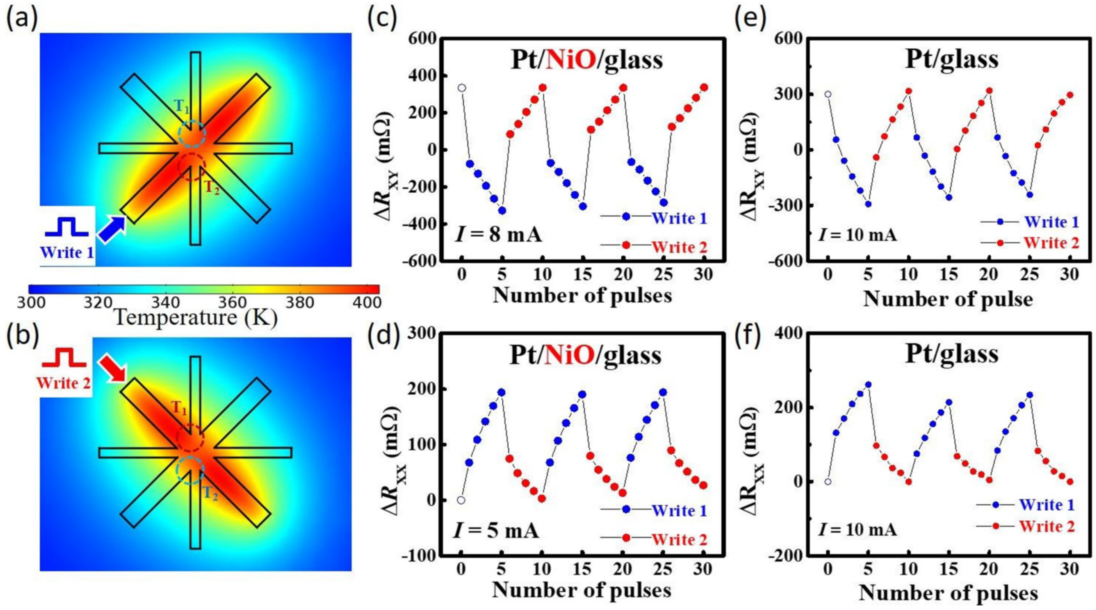

FIG. 4. Simulation of temperature distribution for the eight-terminal patterned Pt/glass structure after applying single pulse current along (a) 45° (write 1) and (b) 135° (write 2) lines. The relative changes of ΔR_{XY} and ΔR_{XX} with and without the AF layer after applying successive writing pulses current alternately along the 45° and the 135° lines for (c) and (d) Pt/NiO/glass and (e) and (f) Pt/glass, respectively. Reproduced with permission from Chiang *et al.*, Phys. Rev. Lett. **123**, 227203 (2019). Copyright 2019 American Physical Society.

break-down value, cause annealing and electromigration, resulting in permanent changes of the microstructures and electrical resistance. The mechanism for electrical switching of Néel vector continues to be debated. It appears that heat generation and dissipation are integral parts of AF switching, if switching happens at all. It has been shown that the intense heat and thermal gradient cause large changes of apparent electrical signals in the same patterned structures, by as much as two orders of magnitude, when placed on different substrates, where the changes scale inversely with the thermal conductivity of substrates.[61] This is unfavorable for any future electronic devices with performance dictated by the substrate and its heat conduction.

MAGNETIZATION-DEPENDENT SPIN HALL EFFECT (MDSHE)

In the conventional SHE, the charge current $\boldsymbol{j}_C$, the spin current $\boldsymbol{j}_S$, and spin index $\boldsymbol{\sigma}$ are mutually perpendicular as shown in Eq. (1). Recent theoretical proposals of interfacial spin–orbit coupling,[64] spin swapping,[65] and the experimental observations of magnetization-dependent surface spin accumulation[66] and spin–orbit torque[50] and the magnetic spin Hall effect[67] suggest that the strict cross-product relation in the conventional SHE may be lifted and be generalized to

$$\boldsymbol{j}_S = (\hbar/2e)\theta_{MDSH}\,\boldsymbol{j}_C \times (\boldsymbol{\sigma} \times \boldsymbol{m}). \tag{3}$$

Experimentally, the unconventional spin accumulation and the resultant SOT may be observed by the SOT switching device,[50] the polar magneto-optic-Kerr-effect measurement,[66] the spin Seebeck effect, the second-order planar Hall effect, and the spin-torque FMR spectroscopy,[68] in the all-metallic Py-based heterostructures. However, as noted above, as long as FM metals with IMA are involved, the propensities of the anomalous Hall effect (AHE) and ANE in the FM metals are unavoidable, and the separation of these parasitic effects is non-trivial.

A better design involves the LSSE measurement in Pt/Co/Pt/YIG, where Pt/Co/Pt with PMA is situated on top of the YIG with IMA as shown in Fig. 5.[69] Under an out-of-plane temperature gradient

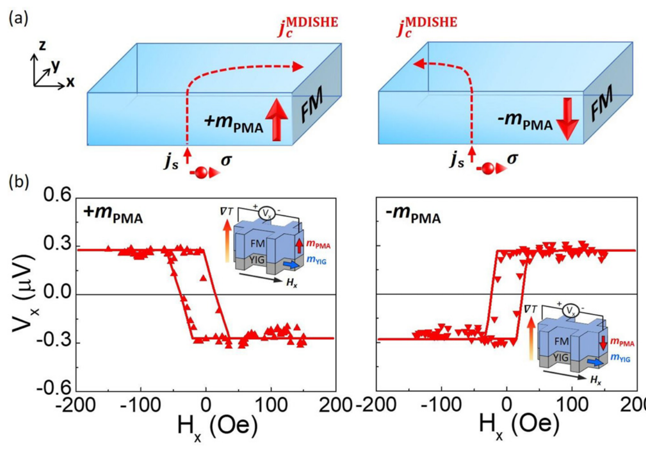

FIG. 5. (a) Schematics of the magnetization-dependent inverse spin Hall effect signal (j_c^{MDISHE}) in the ferromagnet (FM) with perpendicular magnetization ($\boldsymbol{m}_{PMA}$). For simplicity, one polarization (σ) of opposite spins is drawn for the pure spin current ($\boldsymbol{j}_s$). (b) MDISHE voltage for Pt/Co/Pt/YIG with $\boldsymbol{m}_{PMA}$ fixed along $+z$ or $-z$ directions. The insets show the experimental setup with the magnetic field applied and thermal voltage measured both along x. Reproduced with permission from Chuang *et al.*, Phys. Rev. Res. **2**, 032053(R) (2020). Copyright 2020 American Physical Society.

(z-direction), with magnetization of YIG in the y-direction, one measures the ISHE voltage in Pt/Co/Pt in the x-direction, without the contamination of the AHE or ANE with magnetization of Pt/Co/Pt/YIG in the z-direction. When the magnetization of YIG is aligned in the x-direction, there is no ISHE in the x-direction, but only the MDISHE. In this manner, ISHE and MDISHE can be revealed separately and cleanly in the same structure under the same temperature gradient. The ratio of spin Hall angle $\theta_{MDSH}/\theta_{SH}$ is found to be about 3.6%. The MDSHE is a novel and small effect but can be clearly observed. It demonstrates that one can independently control the spin index in spin current by magnetization orientation in the FM layer beyond the strict cross-product relation in the conventional SHE.

SUMMARY

The generation of pure spin current relies on the schemes of the SHE, LSSE, and SP. The injected pure spin current can only be indirectly measured by spin-to-charge conversion via the ISHE, the evidence of which needs to be carefully analyzed to exclude other accompanying effects. We show that the overwhelming ANE in FM metals greatly complicates the detection of pure spin current. The FMIs, without the charge effects, perform much superior for the LSSE but pose additional complications in SP experiments. The intriguing prospect of coherent injection via SP awaits experimental confirmation. SOT switching, a switching mechanism since STT, is readily achieved in the FM with IMA, but not in FM materials with PMA, which are attractive for high-density memory devices. The prospects of electrical switching in AF materials remain tantalizing and controversial. The paramount role of heat is unattractive for applications. Finally, while the SHE features prominently in all pure spin current phenomena with a strict cross product rule, the restriction can be lift by the recently predicted and clearly observed MDSHE.

ACKNOWLEDGMENTS

The work at NTU was supported by the Ministry of Science and Technology of Taiwan under Grant Nos. MOST 106-2628-M-002-015-MY3 and MOST 109-2123-M-002-002. The work at Academia Sinica was supported by the AS Thematic Project No. AS-TP-107-M04 and iMATE Project No. AS-iMATE-109-11. The work at JHU was supported by the U.S. Department of Energy, Basic Energy Science Award No. DE-SC0009390. Weiwei Lin was supported in part by U.S. National Science Foundation DMREF Grant No. 1729555.

DATA AVAILABILITY

The data that support the findings of this study are available from the corresponding author upon reasonable request.

REFERENCES

[1] M. I. Dyakonov and V. I. Perel, "Current-induced spin orientation of electrons in semiconductors," Phys. Lett. A **35**, 459 (1971).
[2] J. E. Hirsch, "Spin Hall effect," Phys. Rev. Lett. **83**, 1834 (1999).
[3] J. Sinova, S. O. Valenzuela, J. Wunderlich, C. H. Back, and T. Jungwirth, "Spin Hall effects," Rev. Mod. Phys. **87**, 1213 (2015).
[4] Y. Tserkovnyak, A. Brataas, and G. E. W. Bauer, "Enhanced gilbert damping in thin ferromagnetic films," Phys. Rev. Lett. **88**, 117601 (2002).
[5] K. Uchida, H. Adachi, T. Ota, H. Nakayama, S. Maekawa, and E. Saitoh, "Observation of longitudinal spin-Seebeck effect in magnetic insulators," Appl. Phys. Lett. **97**, 172505 (2010).
[6] K. Ando, S. Takahashi, K. Harii, K. Sasage, J. Ieda, S. Maekawa, and E. Saitoh, "Electric manipulation of spin relaxation using the spin Hall effect," Phys. Rev. Lett. **101**, 036601 (2008).
[7] L. Liu, C. F. Pai, Y. Li, H. W. Tseng, D. C. Ralph, and R. A. Buhrman, "Spin-torque switching with the giant spin Hall effect of tantalum," Science **336**, 555 (2012).
[8] A. Manchon, J. Železný, I. M. Miron, T. Jungwirth, J. Sinova, A. Thiaville, K. Garello, and P. Gambardella, "Current-induced spin-orbit torques in ferromagnetic and antiferromagnetic systems," Rev. Mod. Phys. **91**, 035004 (2019).
[9] J. C. Slonczewski, "Current-driven excitation of magnetic multilayers," J. Magn. Magn. Mater. **159**, L1 (1996).
[10] L. Berger, "Emission of spin waves by a magnetic multilayer traversed by a current," Phys. Rev. B **54**, 9353 (1996).
[11] C. Hahn, G. de Loubens, O. Klein, M. Viret, V. V. Naletov, and J. Ben Youssef, "Comparative measurements of inverse spin Hall effects and magnetoresistance in YIG/Pt and YIG/Ta," Phys. Rev. B **87**, 174417 (2013).
[12] D. Qu, S. Y. Huang, B. F. Miao, S. X. Huang, and C. L. Chien, "Self-consistent determination of spin Hall angles in selected 5d metals by thermal spin injection," Phys. Rev. B **89**, 140407(R) (2014).
[13] B. F. Miao, S. Y. Huang, D. Qu, and C. L. Chien, "Inverse spin Hall effect in a ferromagnetic metal," Phys. Rev. Lett. **111**, 066602 (2013).
[14] C. Du, H. Wang, F. Yang, and P. C. Hammel, "Systematic variation of spin-orbit coupling with d-orbital filling: Large inverse spin Hall effect in 3d transition metals," Phys. Rev. B **90**, 140407(R) (2014).
[15] D. Qu, S. Y. Huang, and C. L. Chien, "Inverse spin Hall effect in Cr: Independence of antiferromagnetic ordering," Phys. Rev. B **92**, 020418 (R) (2015).
[16] S. Y. Huang, W. G. Wang, S. F. Lee, J. Kwo, and C. L. Chien, "Intrinsic spin-dependent thermal transport," Phys. Rev. Lett. **107**, 216604 (2011).
[17] T. C. Chuang, P. L. Su, P. H. Wu, and S. Y. Huang, "Enhancement of the anomalous Nernst effect in ferromagnetic thin films," Phys. Rev. B **96**, 174406 (2017).
[18] K.-D. Lee, D.-J. Kim, H. Y. Lee, S.-H. Kim, J.-H. Lee, K.-M. Lee, J.-R. Jeong, K.-S. Lee, H.-S. Song, J.-W. Sohn, S.-C. Shin, and B.-G. Park, "Thermoelectric signal enhancement by reconciling the spin Seebeck and anomalous Nernst effects in ferromagnet/non-magnet multilayers," Sci. Rep. **5**, 10249 (2015).
[19] J. Holanda, O. Alves Santos, R. O. Cunha, J. B. S. Mendes, R. L. Rodríguez-Suárez, A. Azevedo, and S. M. Rezende, "Longitudinal spin Seebeck effect in permalloy separated from the anomalous Nernst effect: Theory and experiment," Phys. Rev. B **95**, 214421 (2017).
[20] P. Bougiatioti, C. Klewe, D. Meier, O. Manos, O. Kusche, J. Wollschläger, L. Bouchenoire, S. D. Brown, J.-M. Schmalhorst, G. Reiss, and T. Kuschel, "Quantitative disentanglement of the spin Seebeck, proximity-induced, and ferromagnetic-induced anomalous Nernst effect in normal-metal-ferromagnet bilayers," Phys. Rev. Lett. **119**, 227205 (2017).
[21] H. Kannan, X. Fan, H. Celik, X. Han, and J. Q. Xiao, "Thickness dependence of anomalous Nernst coefficient and longitudinal spin Seebeck effect in ferromagnetic Ni_xFe_{100-x} films," Sci. Rep. **7**, 6175 (2017).
[22] Z. Duan, B. Miao, L. Sun, D. Wu, J. Du, and H. Ding, "The longitudinal spin Seebeck coefficient of Fe," IEEE Magn. Lett. **10**, 1 (2019).
[23] E. Saitoh, M. Ueda, H. Miyajima, and G. Tatara, "Conversion of spin current into charge current at room temperature: Inverse spin-Hall effect," Appl. Phys. Lett. **88**, 182509 (2006).
[24] W. G. Egan and H. J. Juretschke, "DC detection of ferromagnetic resonance in thin nickel films," J. Appl. Phys. **34**, 1477 (1963).
[25] M. Harder, Y. S. Gui, and C. M. Hu, "Electrical detection of magnetization dynamics via spin rectification effects," Phys. Rep. **661**, 1 (2016).
[26] R. Iguchi and E. Saitoh, "Measurement of spin pumping voltage separated from extrinsic microwave effects," J. Phys. Soc. Jpn. **86**, 011003 (2017).
[27] D.-J. Kim, S.-I. Kim, S.-Y. Park, K.-D. Lee, and B.-G. Park, "Ferromagnetic resonance spin pumping in CoFeB with highly resistive non-magnetic electrodes," Curr. Appl. Phys. **14**, 1344 (2014).
[28] R. Yu, B. F. Miao, L. Sun, Q. Liu, J. Du, P. Omelchenko, B. Heinrich, M. Wu, and H. F. Ding, "Determination of spin Hall angle and spin diffusion length in β-phase-dominated tantalum," Phys. Rev. Mater. **2**, 074406 (2018).
[29] P. Deorani and H. Yang, "Role of spin mixing conductance in spin pumping: Enhancement of spin pumping efficiency in Ta/Cu/Py structures," Appl. Phys. Lett. **103**, 232408 (2013).

[30] A. Conca, B. Heinz, M. R. Schweizer, S. Keller, E. T. Papaioannou, and B. Hillebrands, "Lack of correlation between the spin-mixing conductance and the inverse spin Hall effect generated voltages in CoFeB/Pt and CoFeB/Ta bilayers," Phys. Rev. B **95**, 174426 (2017).
[31] J. C. Rojas Sánchez, L. Vila, G. Desfonds, S. Gambarelli, J. P. Attane, J. M. De Teresa, C. Magen, and A. Fert, "Spin-to-charge conversion using Rashba coupling at the interface between non-magnetic materials," Nat. Commun. **4**, 2944 (2013).
[32] D. Yue, W. Lin, J. Li, X. Jin, and C. L. Chien, "Spin-to-charge conversion in Bi films and Bi/Ag bilayers," Phys. Rev. Lett. **121**, 037201 (2018).
[33] C. W. Sandweg, Y. Kajiwara, K. Ando, E. Saitoh, and B. Hillebrands, "Enhancement of the spin pumping efficiency by spin wave mode selection," Appl. Phys. Lett. **97**, 252504 (2010).
[34] Y. S. Chen, J. G. Lin, S. Y. Huang, and C. L. Chien, "Incoherent spin pumping from YIG single crystals," Phys. Rev. B **99**, 220402(R) (2019).
[35] F.-J. Chang, J. G. Lin, and S.-Y. Huang, "Robust spin current generated by the spin Seebeck effect," Phys. Rev. Mater. **1**, 031401(R) (2017).
[36] D. Qu, S. Y. Huang, J. Hu, R. Wu, and C. L. Chien, "Intrinsic spin Seebeck effect in Au/YIG," Phys. Rev. Lett. **110**, 067206 (2013).
[37] D. Tian, Y. Li, D. Qu, S. Y. Huang, X. Jin, and C. L. Chien, "Manipulation of pure spin current in ferromagnetic metals independent of magnetization," Phys. Rev. B. **94**, 020403(R) (2016).
[38] W. Lin, K. Chen, S. Zhang, and C. L. Chien, "Enhancement of thermally injected spin current through an antiferromagnetic insulator," Phys. Rev. Lett. **116**, 186601 (2016).
[39] P.-H. Wu, Y.-C. Tu, D. Qu, H.-L. Liang, S.-F. Lee, and S.-Y. Huang, "Probing the spin-glass freezing transition in $Cu_{1-x}Mn_x$ alloy by spin current," Phys. Rev. B **101**, 104413 (2020).
[40] Z. Qiu, J. Li, D. Hou, E. Arenholz, A. T. N'Diaye, A. Tan, K. Uchida, K. Sato, S. Okamoto, Y. Tserkovnyak, Z. Q. Qiu, and E. Saitoh, "Spin-current probe for phase transition in an insulator," Nat. Commun. **7**, 12670 (2016).
[41] S. Bhatti, R. Sbiaa, A. Hirohata, H. Ohno, S. Fukami, and S. N. Piramanayagam, Mater. Today **20**, 530 (2017).
[42] L. Liu, O. J. Lee, T. J. Gudmundsen, D. C. Ralph, and R. A. Buhrman, "Current-induced switching of perpendicularly magnetized magnetic layers using spin torque from the spin Hall effect," Phys. Rev. Lett. **109**, 096602 (2012).
[43] G. Mihajlovic, O. Mosendz, L. Wan, N. Smith, Y. Choi, Y. Wang, and J. A. Katine, "Pt thickness dependence of spin Hall effect switching of in-plane magnetized CoFeB free layers studied by differential planar Hall effect," Appl. Phys. Lett. **109**, 192404 (2016).
[44] I. M. Miron, K. Garello, G. Gaudin, P. J. Zermatten, M. V. Costache, S. Auffret, S. Bandiera, B. Rodmacq, A. Schuhl, and P. Gambardella, "Perpendicular switching of a single ferromagnetic layer induced by in-plane current injection," Nature **476**, 189 (2011).
[45] S. Fukami, T. Anekawa, C. Zhang, and H. Ohno, "A spin-orbit torque switching scheme with collinear magnetic easy axis and current configuration," Nat. Nanotechnol. **11**, 621 (2016).
[46] G. Yu, P. Upadhyaya, Y. Fan, J. G. Alzate, W. Jiang, K. L. Wong, S. Takei, S. A. Bender, L. T. Chang, Y. Jiang, M. Lang, J. Tang, Y. Wang, Y. Tserkovnyak, P. K. Amiri, and K. L. Wang, "Switching of perpendicular magnetization by spin–orbit torques in the absence of external magnetic fields," Nat. Nanotechnol. **9**, 548 (2014).
[47] L. You, O. Lee, D. Bhowmik, D. Labanowski, J. Hong, J. Bokor, and S. Salahuddin, "Switching of perpendicularly polarized nanomagnets with spin orbit torque without an external magnetic field by engineering a tilted anisotropy," Proc. Natl. Acad. Sci. U. S. A. **112**, 10310 (2015).
[48] S. Fukami, C. Zhang, S. DuttaGupta, A. Kurenkov, and H. Ohno, "Magnetization switching by spin-orbit torque in an antiferromagnet-ferromagnet bilayer system," Nat. Mater. **15**, 535 (2016).
[49] A. van den Brink, G. Vermijs, A. Solignac, J. Koo, J. T. Kohlhepp, H. J. Swagten, and B. Koopmans, "Field-free magnetization reversal by spin-Hall effect and exchange bias," Nat. Commun. **7**, 10854 (2016).
[50] S. C. Baek, V. P. Amin, Y. W. Oh, G. Go, S. J. Lee, G. H. Lee, K. J. Kim, M. D. Stiles, B. G. Park, and K. J. Lee, "Spin currents and spin-orbit torques in ferromagnetic trilayers," Nat. Mater. **17**, 509 (2018).
[51] T. C. Chuang, C. F. Pai, and S. Y. Huang, "Cr-induced perpendicular magnetic anisotropy and field-free spin-orbit-torque switching," Phys. Rev. Appl. **11**, 061005 (2019).
[52] Y. Fan, P. Upadhyaya, X. Kou, M. Lang, S. Takei, Z. Wang, J. Tang, L. He, L.-T. Chang, M. Montazeri, G. Yu, W. Jiang, T. Nie, R. N. Schwartz, Y. Tserkovnyak, and K. L. Wang, "Magnetization switching through giant spin-orbit torque in a magnetically doped topological insulator heterostructure," Nat. Mater. **13**, 699 (2014).
[53] N. H. D. Khang, Y. Ueda, and P. N. Hai, "A conductive topological insulator with large spin Hall effect for ultralow power spin-orbit torque switching," Nat. Mater. **17**, 808 (2018).
[54] M. DC, R. Grassi, J.-Y. Chen, M. Jamali, D. R. Hickey, D. Zhang, Z. Zhao, H. Li, P. Quarterman, Y. Lv, M. Li, A. Manchon, K. A. Mkhoyan, T. Low, and J.-P. Wang, "Room-temperature high spin–orbit torque due to quantum confinement in sputtered $Bi_xSe_{(1-x)}$ films," Nat. Mater. **17**, 800 (2018).
[55] P. Wadley, B. Howells, J. Železný, C. Andrews, V. Hills, R. P. Campion, V. Novák, K. Olejník, F. Maccherozzi, S. S. Dhesi, S. Y. Martin, T. Wagner, J. Wunderlich, F. Freimuth, Y. Mokrousov, J. Kuneš, J. S. Chauhan, M. J. Grzybowski, A. W. Rushforth, K. W. Edmonds, B. L. Gallagher, and T. Jungwirth, "Electrical switching of an antiferromagnet," Science **351**, 587 (2016).
[56] S. Y. Bodnar, L. Šmejkal, I. Turek, T. Jungwirth, O. Gomonay, J. Sinova, A. A. Sapozhnik, H. J. Elmers, M. Kläui, and M. Jourdan, "Writing and reading antiferromagnetic Mn_2Au by Néel spin-orbit torques and large anisotropic magnetoresistance," Nat. Commun. **9**, 348 (2018).
[57] X. Z. Chen, R. Zarzuela, J. Zhang, C. Song, X. F. Zhou, G. Y. Shi, F. Li, H. A. Zhou, W. J. Jiang, F. Pan, and Y. Tserkovnyak, "Antidamping-torque-induced switching in biaxial antiferromagnetic insulators," Phys. Rev. Lett. **120**, 207204 (2018).
[58] L. Baldrati, C. Schmitt, O. Gomonay, R. Lebrun, R. Ramos, E. Saitoh, J. Sinova, and M. Kläui, "Efficient spin torques in antiferromagnetic CoO = Pt quantified by comparing field- and current-induced switching," Phys. Rev. Lett. **125**, 077201 (2020).
[59] P. Zhang, J. Finley, T. Safi, and L. Liu, "Quantitative study on current-induced effect in an antiferromagnet insulator/Pt bilayer film," Phys. Rev. Lett. **123**, 247206 (2019).
[60] Y. Cheng, S. Yu, M. Zhu, J. Hwang, and F. Yang, "Electrical switching of tristate antiferromagnetic Néel order in α-Fe_2O_3 epitaxial films," Phys. Rev. Lett. **124**, 027202 (2020).
[61] C. C. Chiang, S. Y. Huang, D. Qu, P. H. Wu, and C. L. Chien, "Absence of evidence of electrical switching of the antiferromagnetic Néel vector," Phys. Rev. Lett. **123**, 227203 (2019).
[62] A. Churikova, D. Bono, B. Neltner, A. Wittmann, L. Scipioni, A. Shepard, T. Newhouse-Illige, J. Greer, and G. S. D. Beach, "Non-magnetic origin of spin Hall magnetoresistance-like signals in Pt films and epitaxial NiO/Pt bilayers," Appl. Phys. Lett. **116**, 022410 (2020).
[63] T. Matalla-Wagner, J.-M. Schmalhorst, G. Reiss, N. Tamura, and M. Meinert, "Resistive contribution in electrical-switching experiments with antiferromagnets," Phys. Rev. Res. **2**, 033077 (2020).
[64] V. P. Amin and M. D. Stiles, "Spin transport at interfaces with spin-orbit coupling: Formalism," Phys. Rev. B **94**, 104419 (2016).
[65] C. O. Pauyac, M. Chshiev, A. Manchon, and S. A. Nikolaev, "Spin Hall and spin swapping torques in diffusive ferromagnets," Phys. Rev. Lett. **120**, 176802 (2018).
[66] A. M. Humphries, T. Wang, E. R. J. Edwards, S. R. Allen, J. M. Shaw, H. T. Nembach, J. Q. Xiao, T. J. Silva, and X. Fan, "Observation of spin-orbit effects with spin rotation symmetry," Nat. Commun. **8**, 911 (2017).
[67] M. Kimata, H. Chen, K. Kondou, S. Sugimoto, P. K. Muduli, M. Ikhlas, Y. Omori, T. Tomita, A. H. MacDonald, S. Nakatsuji, and Y. Otani, "Magnetic and magnetic inverse spin Hall effects in a non-collinear antiferromagnet," Nature **565**, 627 (2019).
[68] T. Wang, S. Lendinez, M. B. Jungfleisch, J. Kolodzey, J. Q. Xiao, and X. Fan, "Detection of spin-orbit torque with spin rotation symmetry," Appl. Phys. Lett. **116**, 012404 (2020).
[69] T. C. Chuang, D. Qu, S. Y. Huang, and S. F. Lee, "Magnetization-dependent spin Hall effect in a perpendicular magnetized film," Phys. Rev. Res. **2**, 032053 (2020).